JOURNAL OF GEOPHYSICAL RESEARCH, VOL. 101, NO. C3, PAGES 6429–6440, MARCH 15, 1996

Topographic Rossby modes in the Strait of Sicily

Stefano Pierini

Istituto di Meteorologia e Oceanografia, Istituto Universitario Navale, Naples, Italy

Abstract. In this paper, numerical results of a barotropic circulation model are presented, indicating that topographic Rossby modes can be excited in the area of the Strait of Sicily. The results also suggest that such motions are robust features since they can be resonantly generated by different forcings. A numerical barotropic shallow-water model is implemented in the central Mediterranean Sea, and in order to perform a spectroscopic analysis, the initial value problem is solved, both in the presence of a white wind with spatially constant curl and of a white boundary flow representing an equivalent remote pressure forcing. A spectral analysis in selected points in the region of the strait reveals five peaks with periods ranging from 2 to 5 days. The associated circulation patterns are then studied by forcing the system with monochromatic winds or boundary flows at the periods of the energy peaks. Traveling patterns are recognized, whose spatial/temporal structures and periods are found to compare well with those of analytical Rossby modes, thus obtaining a clear evidence of their dynamical nature. In order to investigate the actual excitation of Rossby modes in realistic conditions, the system is then forced by the 1980 National Meteorological Center momentum flux data. The main mode at nearly 3 days obtained from the preceding spectral analysis is indeed found to be excited in the narrowest section of the strait during winter and autumn months. Rossby modes in the numerical time series are identified by means of the analysis of the energy spectra and of the coherence and phase of current signals between two points along the theoretical propagation direction. Finally, the existence of topographic Rossby modes in the Strait of Sicily is discussed in connection with the local properties of horizontal mixing in that area.

1. Introduction

The classical model of barotropic planetary Rossby waves is based on the equation of conservation of potential vorticity in the quasi-geostrophic approximation, in which the variation of the Coriolis force with latitude (the so-called β effect) acts as the restoring force [e.g., *Pedlosky*, 1987]. The infinite β plane case can be extended to a closed domain, this situation being of particular oceanographic interest when the typical horizontal scale of the forcing is comparable to or larger than that of the basin. In such a case the existence of lateral boundary conditions leads to an eigenvalue problem whose solution provides the Rossby (or second class) normal modes of the basin (also called planetary Rossby modes (PRMs)) [e.g., *Pedlosky*, 1965, 1967, 1987; *Longuet-Higgins*, 1964, 1965; *Flierl*, 1977; *Miller*, 1986; *Pierini*, 1990]. Such modes are rotational and basically nondivergent, with no net energy transport within the basin but with phase transport provided by a carrier wave, which can be seen as the result of an appropriate superposition of traveling Rossby waves. The character of the β restoring force is such that the fundamental PRM has the lowest period, and higher modes have increasing periods and smaller and smaller scales, unlike first-class (gravity and inertia gravity) modes, for which smaller scales correspond to higher frequencies.

In the presence of topographic variations an equivalent β effect appears in the conserved potential vorticity, so that one can define a topographic β^* effect. In typical oceans, $|\beta^*|$ may be locally larger or even much larger than $|\beta|$, therefore important modifications are to be expected when topography is taken into account. The effect of idealized shelves, ridges, or seamounts has been considered analytically by *Ripa* [1978]. In the limiting case in which β^* is constant over the basin the problem is qualitatively unchanged, the parameters being suitably scaled; when, on the other hand, confined regions of high values of β^* are present, the modes are trapped in such regions and have generally larger frequencies than in the flat bottom case. In this second case one can speak of topographic Rossby modes (TRMs). Motions of this kind have been obtained in barotropic numerical models of the ocean tides [e.g., *Platzman et al.*, 1981; *Zahel*, 1990; *Ponte*, 1993] and of the Mediterranean Sea [*Candela and Lozano*, 1994]. While topographic Rossby waves have been clearly identified in various oceanic sites [e.g., *Thompson*, 1971; *Thompson and Luyten*, 1976; *Okkonen*, 1993], the only definitive evidence of a TRM in the oceans appears to be that given in a recent study by A. J. Miller et al. (A topographic-

Paper number 95JC03138.
0148-0227/96/95JC-03138$05.00

Rossby mode resonance over the Iceland-Faeroe ridge, submitted to *Journal of Physical Oceanography*, 1995).

In this paper a numerical barotropic shallow-water model implemented in the central Mediterranean Sea with realistic coastlines and topography allows us to identify TRMs inside and in the vicinity of the Strait of Sicily, a particularly important site for the Mediterranean Sea because of its role in controlling the exchange of the Atlantic and Levantine Intermediate Waters and in providing a pathway to atmospheric pressure release between the western and the Levantine basin [e.g., *Manzella et al.*, 1988; *Manzella and La Violette*, 1990; *Moretti et al.*, 1993; *Candela and Lozano*, 1994; N. Pinardi et al., On the interannual variability of the Mediterranean Sea upper ocean circulation, submitted to *Geophysical Research Letters*, 1995].

First, the initial boundary-value problem is solved in the presence (1) of a white wind with spatially constant curl and (2) of a white boundary forcing representing an equivalent remote pressure forcing (section 2). The analysis of the spectra of the kinetic energy density in selected points of the basin is then performed, and five peaks ranging from 2 to 5 days are identified (section 3). The associated circulation patterns are then studied by forcing the system with monochromatic winds or boundary flows at the periods of the energy peaks and by analyzing the response after having reached a repeating cycle. In such a way, TRMs are recognized (section 4). Their spatial and temporal structures are compared with those of idealized quasi-geostrophic normal modes in a rectangular basin with constant β^*, thus obtaining clear evidence of their dynamical nature. Moreover, the theoretical eigenperiods of the analytical model are computed and are found to compare well with the periods obtained by the spectroscopic analysis. These results indicate that the topography and geometry surrounding the Strait of Sicily may support a variety of topographic Rossby modes. Moreover, such motions appear to be robust since they can be resonantly generated by different forcings.

Second, in order to assess whether and when such modes are excited in realistic situations, the system is then forced by the 1980 National Meteorological Center (Washington, D.C.) momentum flux data (section 5). The two main modes obtained from the preceding spectral analysis are indeed found to be excited in winter months. The mode at T=2.7 days is by far the most energetic and has a large signal also in autumn. The identification of Rossby modes in the numerical time series is performed by analyzing the energy spectra and the coherence and phase of current signals in two points along the theoretical propagation direction.

In the conclusions (section 6) the current meter data and the corresponding analysis required in order to obtain an experimental evidence of the existence of TRMs are discussed. The presence of TRMs in the Strait of Sicily is finally considered in connection with the horizontal mixing of waters in that location.

2. The Model

The barotropic component of the motion is studied by means of the shallow-water equations for a homogeneous incompressible fluid [e.g., *Pedlosky*, 1987]:

$$u_t + uu_x + vu_y - fv = -g\eta_x + A_H\nabla^2 u + \frac{(\tau_{w1} - \tau_{b1})}{\rho H}$$

$$v_t + uv_x + vv_y + fu = -g\eta_y + A_H\nabla^2 v + \frac{(\tau_{w2} - \tau_{b2})}{\rho H}$$

$$\eta_t + (Hu)_x + (Hv)_y = 0 \qquad (1)$$

where $\mathbf{u}(\mathbf{x},t)$ is the depth-averaged velocity; $\eta(\mathbf{x},t)$ is the sea surface displacement; ρ is the constant mean density; $f=f_0+\beta y$ is the Coriolis parameter; A_H is the lateral eddy viscosity coefficient; τ_w the wind stress; $\tau_b=\rho C_{Db}|\mathbf{u}|\mathbf{u}$ is the bottom stress and $H=D+\eta-d$, where D is the mean water depth and $d(\mathbf{x})$ is the bottom topography. An explicit finite difference scheme based on the Arakawa C grid was developed for (1) and was used to solve the initial-value problem with vanishing initial conditions and free-slip boundary conditions. The nonlinear terms in (1) were included in some basic runs, and it was found that they are negligible, so that the problem may be assumed as linear, in general, apart from the small bottom friction terms; the linearized version of (1) is therefore used throughout the paper. The horizontal resolution is $\Delta x=\Delta y$=12.5 km which corresponds approximately to 1/8°; the temporal resolution is Δt=8 s, C_{Db}=0.002, $f_0=0.89\times10^{-4}$ rad s^{-1}, and $\beta=1.82\times10^{-11}$ rad m^{-1} s^{-1}) (corresponding to a β plane centered at 37.5°). The eddy viscosity is chosen as A_H=200 m^2 s^{-1}. Figure 1 shows the domain used and the bottom topography, which comes from a University of Miami database and is chosen with the same resolution of the model. All the boundaries are closed, except lines A and B

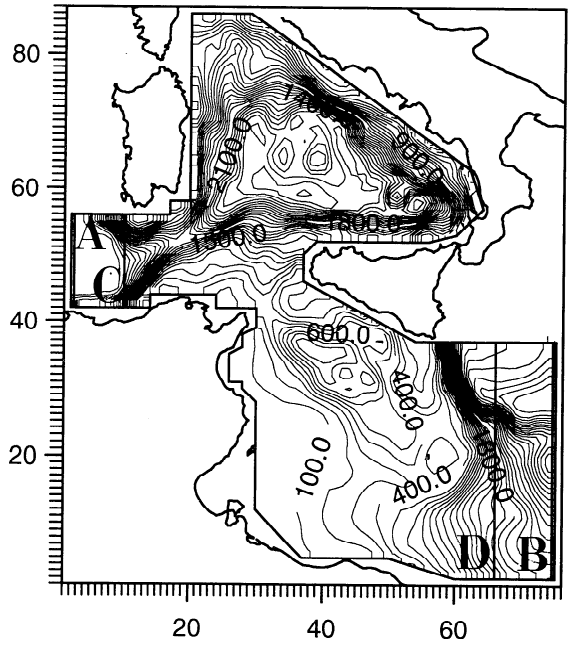

Figure 1. The domain used in the numerical integration and the sea depth in meters. The coordinates are in multiples of the grid step $\Delta x=\Delta y$=12.5 km. Along lines A and B (or, alternatively, C and D) a flow is prescribed in the case of the equivalent pressure forcing. In the wind forcing case they are closed lines.

in the case in which the boundary forcing is considered, where a mass flux is prescribed (see forcing B below).

The equation of conservation of potential vorticity in the quasi-geostrophic approximation, typically used to study Rossby waves, is more restrictive than (1) since it can be derived from (1) under the assumption of small Rossby numbers [e.g., *Pedlosky*, 1987]. Here the more general equations of motion (1) are used because the implicit imposition of the quasi-geostrophic approximation would have limited the generality of the results. Nonetheless, in section 4 the quasi-geostrophic equation will be used to provide a theoretical interpretation of the motions obtained numerically from (1). We now describe the two different forcings used.

Forcing A

The wind stress constitutes the main forcing for barotropic rotational motions in the Mediterranean Sea, although the total wind-driven transport through the Strait of Sicily is found to be weak [*Candela and Lozano*, 1994]. The wind forcing may be, however, a relevant source of energy and vorticity in areas surrounding the strait. In order to perform a spectroscopic analysis aimed at identifying system resonances, the wind stress is taken as a "white" superposition of Fourier components ranging from $T_{\min}$ to $T_{\max}$:

$$\tau(\mathbf{x},t)=\frac{\tilde{\tau}(\mathbf{x})}{N}\sum_{k=1}^{N}\sin(\Omega_k t) \tag{2}$$

where $\Omega_N=2\pi N/T_{\min}$, $\Omega_1=2\pi/T_{\max}$ and $\Omega_k=(k\text{-}1)(\Omega_N-\Omega_1)/(N\text{-}1)+\Omega_1$, with N=500. The wind stress is taken with spatially constant curl:

$$\mathrm{curl}_z\,\tilde{\tau}(\mathbf{x})=\chi=const \tag{3}$$

A wind stress such as (3) represents "large-scale" winds, and this is acceptable in the small region of the Strait of Sicily. Once a peak is identified from the spectra of selected time series, the monochromatic forcing

$$\tau(\mathbf{x},t)=\tilde{\tau}(\mathbf{x})\sin(\overline{\Omega}t) \tag{4}$$

is then used in order to study the response to that particular frequency. Obviously, this procedure is correct thanks to the basic linearity of the problem.

Forcing B

The atmospheric pressure gradients induce in the oceans a nearly inverted barometer response for sufficiently low frequencies (T>2 days), although important deviations from the isostatic adjustment are to be found in regions where modes are excited by the same pressure fluctuations [*Ponte*, 1993] (note that further, though smaller, deviations from isostasy are to be expected in stratified oceans [*Ponte*, 1992]). The associated velocity field is basically barotropic, mainly irrotational, and usually weak. However, owing to the specific geometry of the Mediterranean, such a weak current within the eastern and western Mediterranean basins produces a stronger barotropic signal in the narrow and shallow Strait of Sicily, where therefore this component of the motion results as remotely forced. Moreover, the presence of bottom friction and the interaction of the flow with variable topography can generate rotational motions in this region [*Candela and Lozano*, 1994]. In order to represent the effect of the pressure, which, as just noticed, is substantially remote for the region of interest, the system is forced by prescribed flows through "open" western and eastern boundaries (lines A and B), while no direct meteorological forcings are considered. Such boundary forcing can be seen as the flow produced east and west of the strait by pressure gradients over the two major subbasins. The prescribed volume flux per unit width $\tilde{\mathbf{Q}}=(\tilde{Q}_1,\tilde{Q}_2)$ along A and B is chosen as independent on y and can be specified by an assigned velocity $\tilde{u}(\mathbf{x}_o)$ at a given boundary point $\mathbf{x}_0$ as follows:

$$\tilde{Q}_1\big|_A\equiv\tilde{Q}=\tilde{u}(\mathbf{x}_o)H(\mathbf{x}_o),\quad \tilde{Q}_1\big|_B=\frac{L_A}{L_B}\tilde{Q}$$
$$\tilde{Q}_2\big|_A=\tilde{Q}_2\big|_B=0 \tag{5}$$

where L_A and L_B are the lengths of the lateral boundaries. As for forcing A, a white superposition of Fourier components is considered,

$$Q_1(t)\big|_A=\frac{\tilde{Q}}{N}\sum_{k=1}^{N}\sin(\Omega_k t)$$
$$Q_1(t)\big|_B=\frac{L_A}{L_B}\frac{\tilde{Q}}{N}\sum_{k=1}^{N}\sin(\Omega_k t+\varphi) \tag{6}$$

and after the identification of a resonance at $\overline{\Omega}$ the system is excited by the monochromatic forcing:

$$Q_1(t)\big|_A=\tilde{Q}\sin(\overline{\Omega}t)$$
$$Q_1(t)\big|_B=\frac{L_A}{L_B}\tilde{Q}\sin(\overline{\Omega}t+\varphi) \tag{7}$$

3. The Identification of Energy Peaks

The system is first forced by the wind according to (2) and (3) with χ=4.65x10^{-8} dyn cm^{-3} (a correct order of magnitude for the Mediterranean Sea area), $T_{\min}$=2 days and $T_{\max}$=10 days. The equivalent pressure forcing (6) is then considered with $\tilde{u}(\mathbf{x}_o)$=0.1 m s^{-1} (where $\mathbf{x}_o$ is at the northern boundary of line A) and with four different choices of the phase as follows: $\varphi=0, \pi/2, \pi, 3\pi/2$. The spectra of the kinetic energy density relative to time series taken at three selected points (see Figure 2) are shown in Figures 3 and 4 for the wind and the equivalent pressure forcing, respectively.

Two large peaks at T_1=2.1 days and T_2=2.7 days are present for the wind forcing at P3 (i.e., in the narrowest section of the strait; note the different scale in the spectra for this point), they are still present at P2 (farther north) but with a smaller energy, while they are absent at P1 (even farther north). This indicates that the associated motions are concentrated within the strait. The same peaks appear also for the equivalent pressure forcing and with a similar spatial behavior, but their relative amplitude varies, depending on the east-west phase difference in the boundary

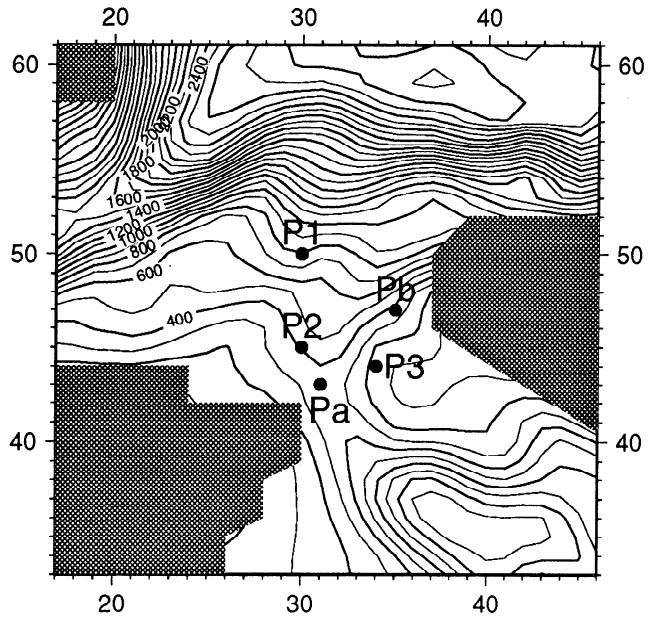

Figure 2. Portion of the domain of integration with sea depth. Points P1, P2, and P3 indicate the locations where the spectroscopic analysis has been carried out. Points Pa and Pb are used in the cross-spectral analysis of section 5.

forcing. The peak at T_2 is always very large, while that at T_1 has a comparable amplitude only for $\varphi=\pi/2$. The resonance at T_2 appears therefore as the most energetic one in this spectral analysis.

The remaining peaks are 1 order of magnitude smaller. Two peaks at T_3=3.7 days and T_4=5.1 days are present, with larger amplitudes at P2. For the equivalent pressure forcing the maximum amplitudes are found for $\varphi=3/2\ \pi$, while the peak at T_4 is not well resolved in the wind forcing case. The signal is weaker at P1 and P3, thus indicating that the corresponding motion is concentrated off the western Sicilian coasts, north of Tunisia.

Finally, a large peak is found at T_5=2.2 days at P1, while it is masked at P2 and P3. Therefore the associated motion is expected to be confined well north of Tunisia. Note that T_5 is very close to T_1; nonetheless, it is clear that the two periods correspond to different motions because the large peak amplitude at P3 at T_1 (see Figures 3 and 4b) decreases notably at P2, while a larger peak appears farther north at T_5. In other words, the small frequency difference is, however, accompanied by a clear spatial separation.

Also in this case, as in all the others, the localization of the peak is the same for both forcings, and this is the first evidence that the associated motions are normal modes of the system that are easily excited by different forcings. In this respect, a third forcing was used (results not shown); a wind setup was produced by a constant wind (with closed lines A and B) that was then switched off. The resulting conversion of potential to kinetic energy leads to peaks in the energy spectra that correspond exactly to those presented above.

It should be noticed that lines A and B in the integration domain, being artificial, were chosen sufficiently far from the region of interest (the Strait of Sicily) in order to reduce their effect on the interior response. However, an analysis is worth carrying out to check how sensitive the response is to the choice of such lines. Figure 5 shows the spectral kinetic energy density for both the wind (Figure 5a; compare with Figure 3) and the remote pressure forcing for $\varphi=\pi$ (Figure 5b; compare with Figure 4c) when lines A and B are substituted by C and D, respectively (see Figure 1). The only consequence of this reduction of the latitudinal extent of the domain is a decrease of the response by 20-50%, but the frequencies associated with each peak do not change at all. As a result, the periods identified in this section are robust to changes in the choice of the artificial boundaries in the Strait of Sardinia and in the Ionian Sea. Lines A and B are, of course, to be considered a better choice than C and D. Naturally, if such boundaries were taken closer and closer to the strait, one would eventually expect the periods to depend more and more on the location of the boundaries.

4. Interpretation of the Circulation Patterns in Terms of Topographic Rossby Modes

In order to analyze the dynamics associated with each of the peaks of kinetic energy identified in the preceding section, the system is forced separately at $\Omega_i = 2\pi / T_i$ (i=1,5) according to (4) with the same χ as in section 3 and to (7) with the same $\tilde{u}(\mathbf{x}_o)$ as in section 3 and with $\varphi=3/2\ \pi$ for T_3 and T_4, with $\varphi=\pi/2$ for T_1 and T_2, and with $\varphi=\pi$ for T_5. The solutions for the two different forcings are similar, apart from a phase difference, therefore only the results relative to the wind forcing are presented. Qualitative and quantitative considerations will also be discussed to support the hypothesis that the flows associated to $T_{1,2,3,4,5}$ are local TRMs.

Let us start by considering the flow associated with the period T_2, corresponding to the main peak in the kinetic energy spectra. The analysis is carried out throughout a

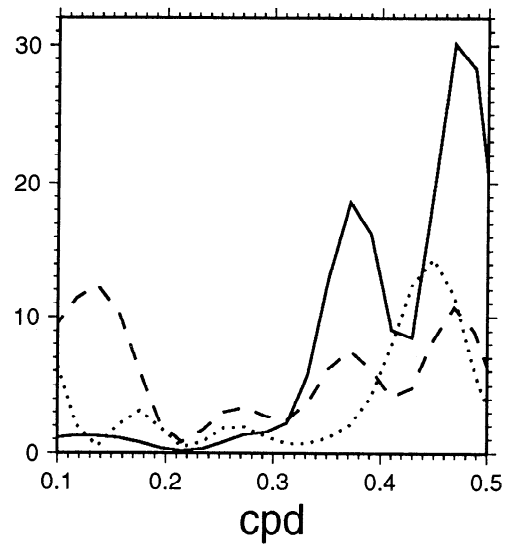

Figure 3. Spectral kinetic energy density versus frequency for the wind forcing case at points P1 (dotted line), P2 (dashed line), and P3 (solid line, multiplied by 10^{-1}). The frequency is in cycles per day (cpd), and y is in $m^3\ s^{-2}\ cpd^{-1}$.

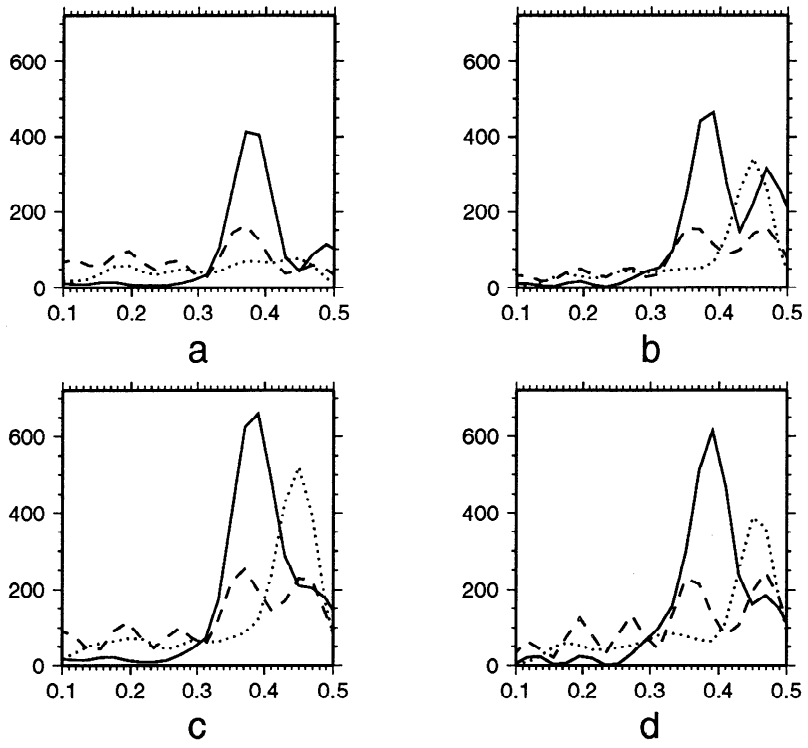

Figure 4. Spectral kinetic energy density versus frequency for the boundary forcing case at points P1 (dotted line), P2 (dashed line), and P3 (solid line, multiplied by 10^{-1}) for phases (a) $\varphi=0$, (b) $\varphi=\pi/2$, (c) $\varphi=\pi$, and (d) $\varphi=3/2\ \pi$. The frequency is in cycles per day, and y is in $m^3\ s^{-2}\ cpd^{-1}$.

complete cycle, after having reached a repeating cycle in the numerical integration. The first thing to be noticed, which is common to all the other cases, is that the currents are virtually parallel to the isobars and are horizontally nondivergent to a good approximation, with a kinetic-to-potential energy ratio of $O(10^3)$. This is typical of quasi-geostrophic flows, and indeed the geostrophic balance between η and **u** can be easily checked by direct computations (a small deviation from geostrophy is due to the Ekman transport, which is superimposed on the virtually geostrophic pressure-driven velocity to give the total **u** produced by the model). The elevation field η is therefore the stream function of the flow and is plotted in subsequent figures in order to show two-dimensional circulation patterns (an appropriate offset is introduced in each picture so as to distinguish between regions of cyclonic and anticyclonic circulation). In Figure 6a a whole cycle is shown relative to T_2 after five cycles from $t=0$

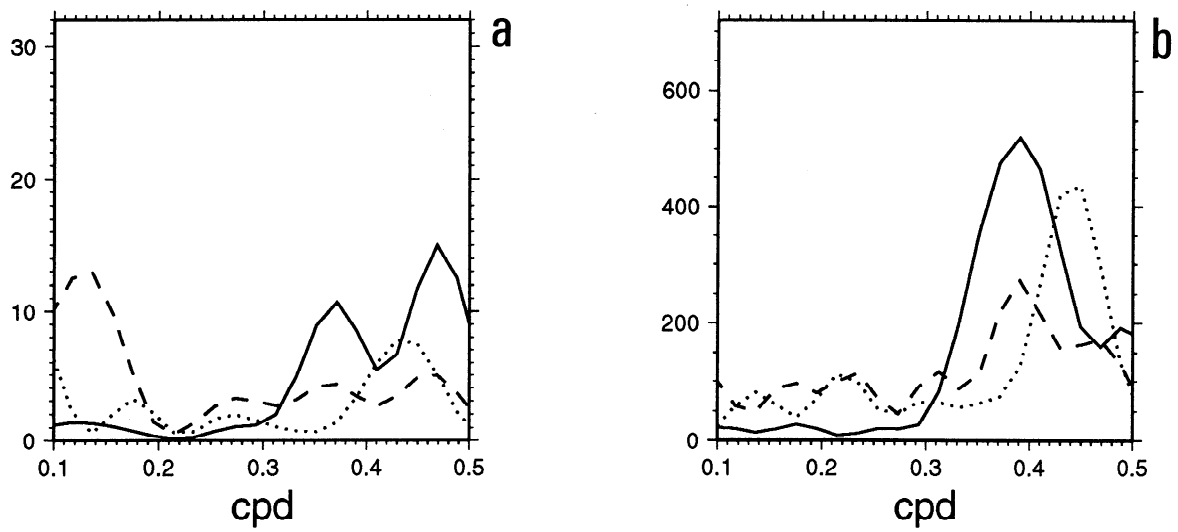

Figure 5. Spectral kinetic energy densities when lines A and B are substituted by C and D, respectively, for (a) wind forcing case (compare with Figure 3) and (b) remote pressure forcing case with $\varphi=\pi$ (compare with Figure 4c) .

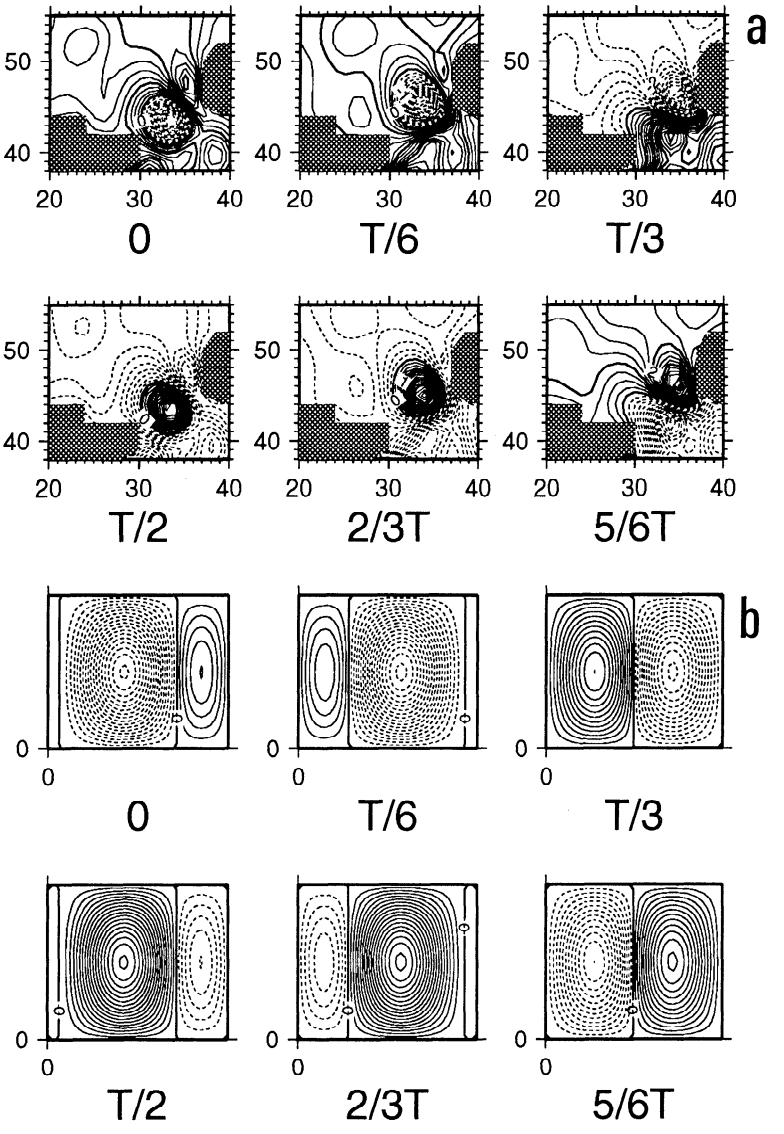

Figure 6. (a) Snapshots of the elevation field (in millimeters) of the topographic Rossby mode associated with the period T_2=2.7 days. A whole cycle is described at times indicated (T is the period). An arbitrary initial phase is considered. (b) First Rossby mode according to equation (8). The parameter values are irrelevant.

(well after spin-up; see end of section 4). It appears that the current patterns are traveling features moving along the southwest/northeast topographic slope in the narrowest section of the strait (see Figure 2). Moreover, the flow is essentially in the form of a positive and a negative vortice smoothly exiting and entering the region.

These are all symptoms that the flow under consideration is the first TRM (section 1), supported by the above mentioned topographic variation and constricted laterally, along the propagation direction, by the Tunisian and the Sicilian coasts and, in the normal direction, by larger values of the topographic gradients. This is confirmed by a comparison with Figure 6b in which the first Rossby mode is shown according to the formula [*Pedlosky*, 1987, section 3.25]:

$$\psi = \cos\left[\frac{\beta x}{2\omega_{mn}} + \omega_{mn} t\right] \sin m\pi \frac{x}{L_x} \sin n\pi \frac{y}{L_y} \qquad (8)$$

with m=n=1 and with an appropriate β which, as we will see below, represents essentially a topographic β effect.

In order to explain theoretically the period T_2, let us consider the equation of conservation of potential vorticity in its quasi-geostrophic, nondivergent, and linearized form [*Pedlosky*, 1987]:

$$\frac{\partial}{\partial t}\nabla^2\psi + \left(\beta + \frac{f_o}{D} d_y\right)\psi_x - \left(\frac{f_o}{D} d_x\right)\psi_y = 0 \qquad (9)$$

where $\psi = (g/f_o)\eta$ is the stream function of the flow. The planetary β effect is accompanied by the topographic β effect represented by

$$\vec{\beta}^* = \frac{f_o}{D}\nabla d$$

In Figure 7 $|\vec{\beta}^*|$ is reported for D=500 m, typical for the region of the Strait of Sicily (units are in 10^{-11} rad m^{-1}s^{-1}).

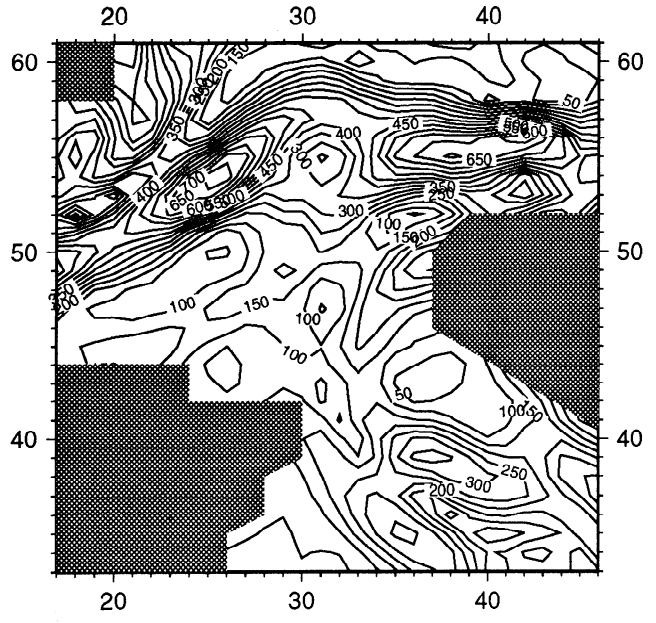

Figure 7. Amplitude of topographic β effect $|\vec{\beta}^*|$ in 10^{-11} rad m^{-1} s^{-1}.

Remembering that $\beta=1.82\times10^{-11}$ rad $m^{-1}s^{-1}$ it is easy to check that

$$|\vec{\beta}^*| \geq O(10^2\,\beta)$$

so that in the region of interest the planetary β effect is totally negligible with respect to the topographic one. In general, the importance of the topographic β effect in typical Mediterranean subbasins was recognized by *Malanotte-Rizzoli and Bergamasco* [1989]. In fact, the topographic variations associated with the shelf and slope regions of the Mediterranean are comparable with those of large oceans, but because of the limited extent of the basins, there are virtually no regions with small ∇d, so that the barotropic circulation is essentially controlled by the topography. In this respect, the inclusion of a realistic topography in circulation models of the Mediterranean turns out to be essential in order to avoid spurious PRMs [S. Pierini, manuscript in preparation, 1996).

Note that for T_2 the mean depth gradient forms an angle of about -45° with respect to y, therefore in this rotated coordinate system, $d_x\cong0$, $\vec{\beta}^* \cong (0,\beta^*)$ and the equation that TRMs should satisfy in our case is approximately given by

$$\frac{\partial}{\partial t}\nabla^2\psi + \beta^*\psi_x = 0 \qquad (10)$$

with $\beta^*<0$ (in agreement with the northeast propagation). Equation (10) with constant β^* has the following dispersion relation for Rossby waves traveling along x:

$$\omega = -\frac{\beta^*}{k} \qquad (11)$$

In a closed rectangular domain the wavenumber k is quantized in order to satisfy the lateral boundary conditions as follows:

$$k_{xm} = \frac{2\pi m}{L_x},\quad k_{yn} = \frac{2\pi n}{L_y} \qquad (12)$$

Substituting (12) into (11), one gets the eigenfrequencies of the TRMs in a rectangular basin with constant β^* [*Pedlosky*, 1987]:

$$\omega_{m,n} = -\frac{\beta^*}{\sqrt{k_{xm}^2 + k_{yn}^2}} \qquad (13)$$

The topographic β effect is certainly not constant in our case; however, its variance is relatively small in the region of propagation of the waves (Figure 7), so the application of the analytical model (13) appears justified in order to obtain a quantitative confirmation of our hypothesis. From the spectroscopic analysis we obtained an eigenperiod T_2=2.7 days, scales $L_x\cong L_y\cong$120 km (Figure 6a), and the indication that the mode should be the lowest one, i.e., $n=m=1$. Substituting these values into (13), one gets the theoretical value

$$|\beta^*| \cong 200\cdot10^{-11} \text{ rad m}^{-1}\text{s}^{-1}$$

which is a correct mean value for β^* in the region under investigation (Figure 7). This constitutes a confirmation of the hypothesis on TRMs.

It should be noticed that (10) should, in principle, include a term that takes into account the small horizontal divergence allowed by the presence of the free surface, which is intrinsic of the shallow-water equations (1). However, in our case the horizontal length scale L is smaller than the external Rossby deformation radius $R=(gD)^{1/2}/f_o$, so that the nondivergent approximation for Rossby modes is fully justified [*Flierl*, 1977; *Pierini*, 1990].

For the remaining four peaks the same arguments based on the application of (13) can be applied, and in all cases a good agreement between numerical and analytical eigenperiods is found. The modes at T_1 and T_5 are the ground states ($n=m=1$) relative to two different domains (as described in section 3). Figure 8a shows that the circulation patterns associated with T_1 are in the form of the first TRM, supported by the strong north-south increase in depth confined between Tunisia and the southwestern Sicilian coasts with nearly horizontal isobaths. Figure 8b shows that also for T_5, one has a first TRM. As expected (section 3), the motion is extended well north of Tunisia and is supported by the relatively smooth, steep depth increase toward the Tyrrhenian Sea. For T_5 the eastern and southern boundaries are given by the Sicilian and the Tunisian coasts, while the northern and western "boundaries" are composed of regions of sharp increases of β^* at the edge of the slope.

The peaks at T_3 and T_4 are the first and second modes, supported by the topographic gradient represented by the shelf slope off the northern Tunisian coasts (Figures 9a and 9b). They are constricted latitudinally by the sharp depth increase in the Strait of Sardinia and by the western Sicilian coast and meridionally by the Tunisian coast and by the northern sharp increase of β^*. Note the double-gyre structure of the second mode at T_4. It is also interesting to notice that with the choices $\beta^*=-150\times10^{-11}$ rad $m^{-1}s^{-1}$,

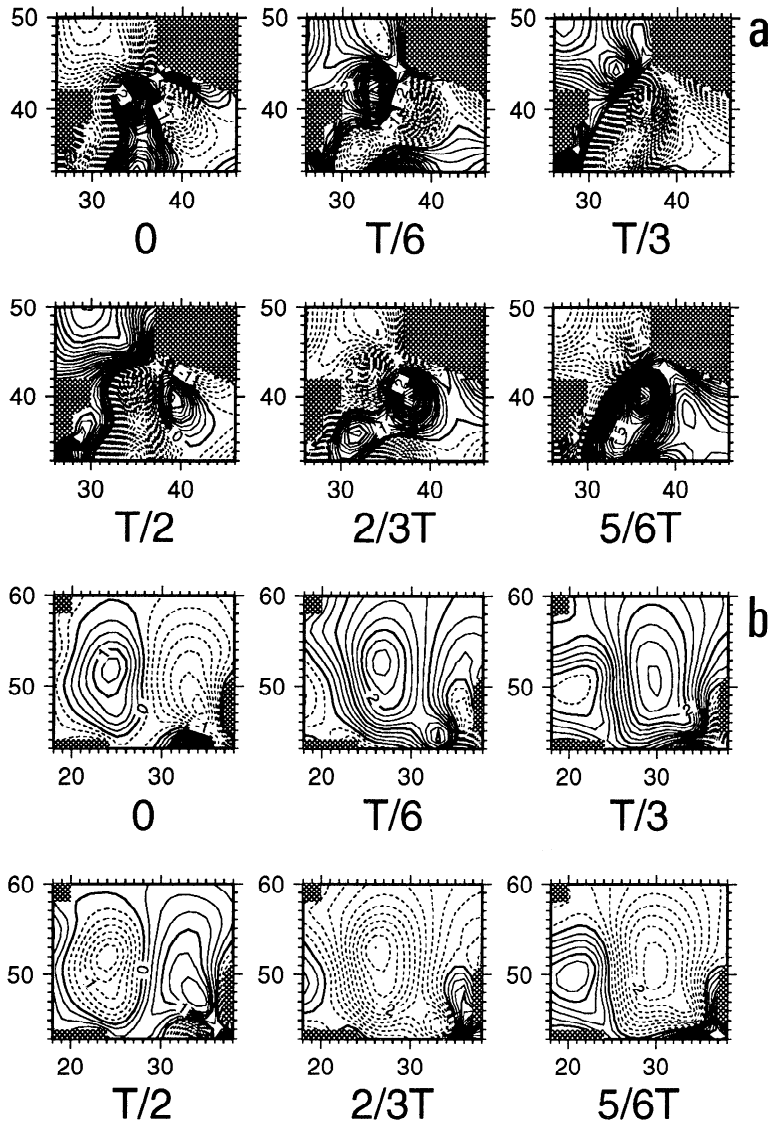

Figure 8. Snapshots of the elevation field (in millimeters) of the topographic Rossby modes associated with the periods (a) T_1=2.1 and (b) T_5=2.2 days. A whole cycle is described at times indicated. An arbitrary initial phase is considered.

L_x=190 km, and L_y=100 km (see Figure 7), the theoretical eigenperiod with m=n=1 approximates T_3 by less then 5%, and with m=2 (second mode) and n=1 it approximates T_4 by less than 10%. This is a further confirmation of the validity of the hypothesis on TRMs.

It is to be stressed that the theoretical model for a closed domain with constant β^* is in good agreement with the numerical circulation model in which each TRM is confined in a semiopen domain, with nearly constant β^* in the interior but with lateral regions with strong variations of β^* (as in all cases considered). From this, one can deduce that regions of large β^* gradients act as rigid boundaries as far as the establishment of TRMs is concerned.

Finally, in order to get visual information on the amplitude of the induced currents, Figure 10 gives an example of the x and y components of the current velocities at P3 for the monochromatic wind forcing case at T_1=2.1 days. First of all, the time series show a rapid spin-up process, leading to a repeating cycle after only two to three cycles. Moreover, for the wind stress curl used (whose order of magnitude is typical for the region of interest) the induced currents have values comparable with those of the local mean flows. From this spectral analysis one can therefore expect that a realistic wind forcing should be able to excite TRMs with an energy not negligible with respect to that of other forms of motion in the same frequency range. In the next section the use of a realistic wind forcing will clarify this point.

5. Analysis of the Response to a Realistic Wind forcing

In this section we study the response of the system to a realistic wind forcing in order to investigate the actual excitation of the modes discussed in the preceding sections. We use the 1980 National Meteorological Center momentum flux data. Their spatial and temporal resolution is 1°x1° and 12 hours, respectively. A smooth wind forcing

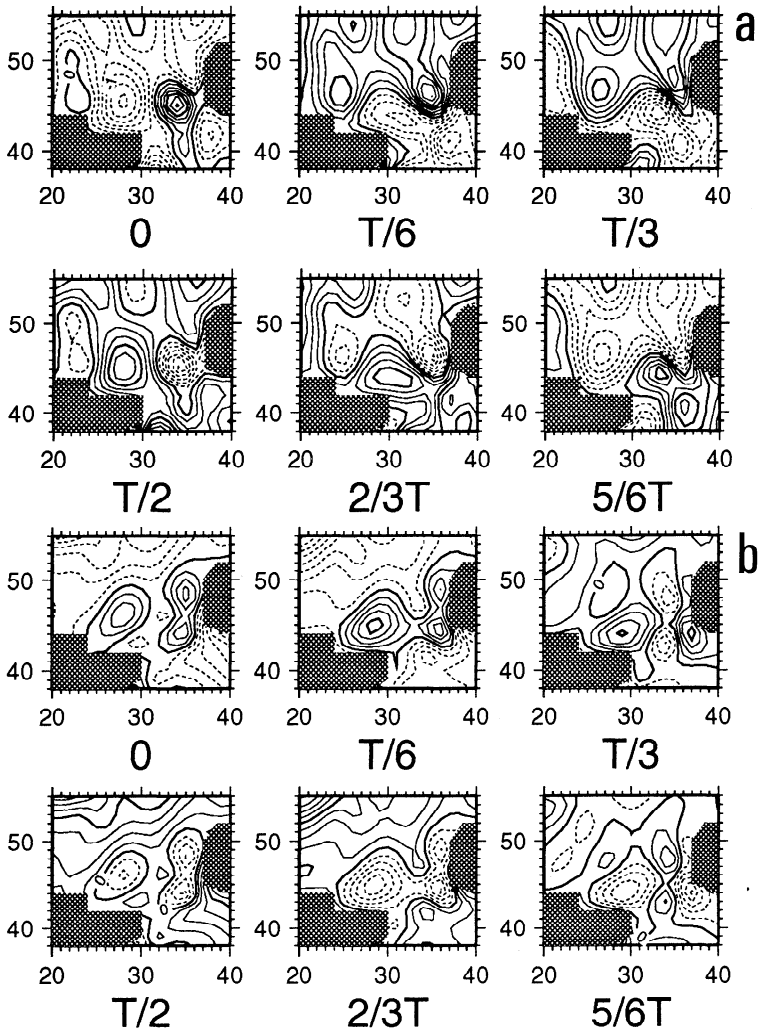

Figure 9. Snapshots of the elevation field (in millimeters) of the topographic Rossby modes associated with the periods (a) T_3=3.7 and (b) T_4=5.1 days. A whole cycle is described at times indicated. An arbitrary initial phase is considered..

is constructed by performing a bilinear interpolation over the regular model grid at each sampling time and then by linearly interpolating the winds at intermediate times.

Let us focus on the response in the narrowest section of the Strait of Sicily (point P3), where the main modes are expected to be excited. In Figure 11 the spectra of the local wind stress curl and of the kinetic energy of the flow are reported for following three different periods of the year: January-February, June-July, and October-November. In winter months (Figure 11, solid lines), two large peaks are present in the flow energy spectra, the largest one at exactly T_2=2.7 days and a broad one at T=3 days. In the local wind stress curl spectrum an analogous broad peak at 3 days is present, suggesting that the corresponding current signal is a direct manifestation of the local wind system. On the contrary, no significant peak near T_2 can be found in the wind stress curl, therefore one can deduce that the TRM corresponding to T_2 (the most energetic one from the spectral analysis of sections 3 and 4) is indeed excited in the winter of the considered forcing. Other energy peaks, in particular, one at T_1, are also present, but they are less significant. In summer (Figure 11, dashed lines), winds and induced currents are weak and without any particular structure. In autumn (Figure 11, dotted lines), on the other hand, a strong peak at T_2 is again present in the flow, while it is absent in the wind. In conclusion, from the analyses of the wind stress curl and of the current kinetic energy spectra the TRM at T_2 appears to be excited during winter and autumn months in the test year 1980.

In order to obtain a more definitive confirmation of this hypothesis, we now consider the January-February time series and the cross-spectra relative to two points (Pa and Pb of Figure 2) taken along the theoretical propagation direction of the mode (see Figure 6a). In Figure 12 the local wind stress curl and the u component of the current velocity (the most significant for the T_2 mode) at points Pa and Pb are presented as a function of time (t=0 corresponds to January 1). First of all, during the first week one can notice two, large, 3-day-period oscillations in both points, presumably forced by the two peaks evident in the wind stress curl (see the preceding discussion on the forced character of the 3-day peak). On January 14 a spike of the wind curl can be observed. This clearly induces in both points a series of four to five free oscillations (this being

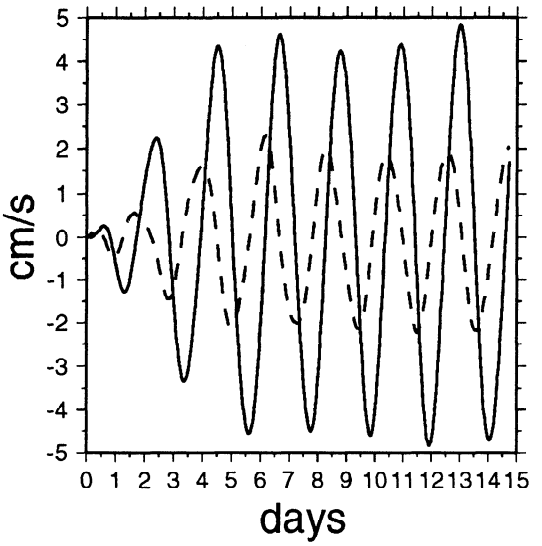

Figure 10. Times series of velocity components u (solid line) and v (dashed line) at points P3 (see Figure 2) for the monochromatic wind forcing at T_1. The wind stress in (4) has a curl given by $\chi=4.65\times10^{-8}$ dyn cm^{-3} (see (3)), representing a correct order of magnitude for the Mediterranean Sea area.

indicative of the dissipation rate of the mode) of period T_2 modulated by a higher-frequency signal. A finer analysis indicates that the latter is in phase at Pa and Pb, whereas for the T_2 oscillations the signal has its first crest at Pa at $t\cong16.8$ days and at Pb at $t\cong18.3$ days. Therefore point Pa leads point Pb by $\cong1.5$ days or 200°. In other words, while the high-frequency signal yields no appreciable phase propagation, being presumably related to first-class modes, for T_2 a southwest/northeast propagation is present, in agreement with the theory presented in this paper. Also in agreement is the time lag; in fact, from Figure 6a it is clear that for the T_2 TRM, the phase at Pb equals that at Pa after a little more than $T/2$ (i.e., $\approx$ 200°).

This empirical determination of the time lag is confirmed by a cross-spectral analysis. In Figure 12 the coherence and phase of u between points Pb and Pa are reported. There is significant coherence at around 1 day and about T_2 (note that the peak maximum is slightly shifted to lower frequencies because a cross-spectral analysis on such a small number of oscillations cannot resolve the two main peaks of Figure 11). The phase is nearly zero around 1 cpd, while it is about -160° (or 200°) at T_2. These considerations provide clear evidence of the excitation of the main TRM in the Strait of Sicily.

6. Conclusions

In this paper, numerical results of a circulation model suggest the possible existence of topographic Rossby modes in the Strait of Sicily and its surroundings. These are traveling rotational normal modes over steep topographic variations delimited horizontally by coasts and by sharp variations of the topographic β effect, have relatively high eigenfrequencies (periods from 2 to 5 days), and can be excited resonantly by either a large-scale wind stress curl or by currents interacting with the topography. A spectroscopic analysis has provided the periods and circulation patterns of the modes. The response to a realistic wind forcing has then revealed the actual excitation of the main mode in the strait, particularly during winter and autumn months.

The inclusion of effects that are neglected in the present study can lead to modifications in the Rossby modes. For instance, the inclusion of baroclinicity would, in conjunction with topographic variations, induce a further barotropic component, though presumably of secondary importance. The incorporation in the model of "mean" flows that are indeed present in the region (i.e., Atlantic and Levantine Intermediate Waters flowing through the strait) would Doppler shift the eigenfrequencies and modify, to some extent, the structure of the modes. Moreover, an increased resolution of the model, accompanied by an analogous increase in the resolution of the bottom topography, could lead to a shift in the eigenperiods and, possibly, to the appearence of higher-order modes not resolved by the present model.

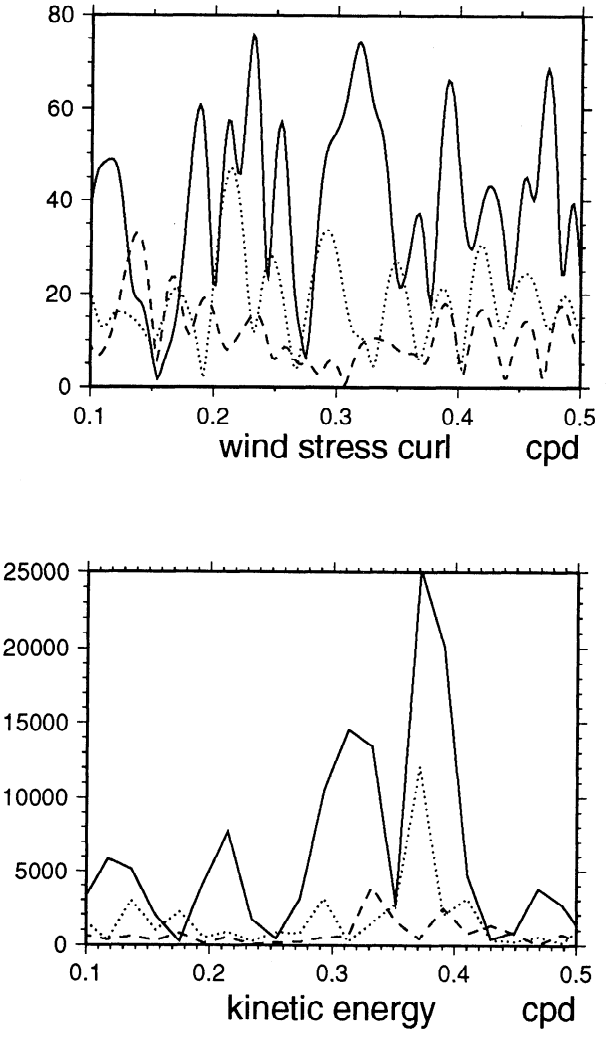

Figure 11. Spectra of the 1980 National Meteorological Center (top) wind stress curl in the Strait of Sicily and (bottom) of the kinetic energy of the flow at point P3 for the periods January-February (solid lines), June-July (dashed lines), and October-November (dotted lines).

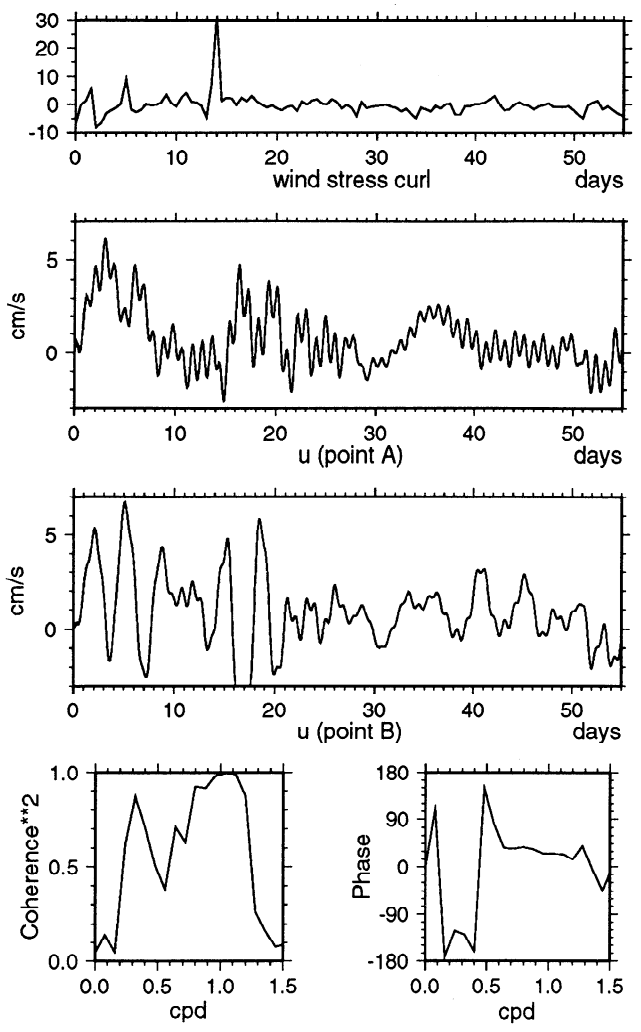

Figure 12. Time series of the National Meteorological Center wind stress curl in the Strait of Sicily (10^{-8} dyn cm^{-3}) and of the u component of the current velocity at points Pa and Pb (see Figure 2) for the period January-February 1980 (t=0 corresponds to January 1). Squared coherence and phase of u relative to Pb and Pa are also given for the same period.

The analysis of available current time series relative to the region under investigation appears to be consistent with the theory presented in this paper (Astraldi, Budillon, Gasparini, Moretti and Sansone, private communications, 1995). Indeed, single-point current meter data reveal series of oscillations with a 3-day period (very close to that of the main theoretical mode) and with amplitudes and dissipation rates comparable to those derived in section 5. However, the identification of periodicities in single-point signals does not provide unambiguous experimental evidence of TRMs. To achieve this, the propagating character of such dynamical features should be properly taken into account, for instance, by collecting data in at least two different locations along the isobaths that are shown to support the modes and by performing a cross-spectral analysis (such as that carried out in section 5), which could then allow detection of Rossby wave propagation.

The TRM contribution to the transport through the Strait of Sicily is concentrated at such high frequencies that the existence of these modes is irrelevant for what concerns long-term variabilities of the total barotropic transport. On the other hand, the excitation of rotational modes with the characteristics of those presented in this paper can be important in determining the horizontal mixing of waters in the region of the Strait of Sicily. This is because strongly inhomogeneous and time-dependent rotational motions produce, in general, what is called chaotic advection, which is a particular form of a shear dispersion phenomenon strictly related to the instability of Lagrangian trajectories. In this respect, the dispersion properties of passive tracers in topographic Rossby modes was recently considered by S. Pierini and E. Zambianchi (manuscript in preparation, 1996). An analytical model for wind-driven Rossby waves in a closed domain was used as the advective field in the reconstruction of Lagrangian trajectories. The flow is indeed found to produce chaotic advection. In addition, a parameterization of turbulence with finite autocorrelation time was also considered, so that the combined effect of chaotic advection and turbulent diffusion could be analyzed. As a result, it can be inferred that the presence of topographic Rossby modes in the Strait of Sicily could make an important contribution to the total mixing in the region.

Acknowledgments. This work was supported by the Comitato Nazionale per le Scienze Fisiche of the Consiglio Nazionale delle Ricerche of Italy. The author wishes to thank E. Zambianchi for helpful discussions. The use of the National Meteorological Center (Washington, D.C.) momentum flux data and of the GMT-System graphics software (Scripps Institution of Oceanography) is kindly acknowledged.

References

Candela, J., and C. J. Lozano, Barotropic response of the western mediterranean to observed atmospheric pressure forcing, in *Seasonal and Interannual Variability of the Western Mediterranean Sea, Coastal Estuarine Stud.*, vol. 46, edited by P. La Violette, pp. 325-359, AGU, Washington, D.C., 1994.

Flierl, G. R., Simple applications of McWilliams' "A note on a consistent quasigeostrophic model in a multiply connected domain," *Dyn. Atmos. Oceans*, *1*, 443-453, 1977.

Longuet-Higgins, M. S., Planetary waves on a rotating sphere, I, *Proc. R. Soc. London A, 279*, 446-473, 1964.

Longuet-Higgins, M. S., Planetary waves on a rotating sphere, II, *Proc. R. Soc. London A, 284*, 40-54, 1965.

Malanotte-Rizzoli, P., and A. Bergamasco, The circulation of the Eastern Mediterranean, I, *Oceanol. Acta*, *12*, 335-351, 1989.

Manzella, G. M. R., and P. E. La Violette, The seasonal variation of water mass content in the western Mediterranean and its relationship with the inflows through the straits of Gibraltar and Sicily, *J. Geophys. Res.*, *95*, 1623-1626, 1990.

Manzella, G. M. R., G. Gasparini, and M. Astraldi, Water exchange between the eastern and western Mediterranean through the strait of Sicily, *Deep Sea Res., Part A, 35*, 1021-1035, 1988.

Miller, A. J., Nondivergent planetary oscillations in midlatitude ocean basins with continental shelves, *J. Phys. Oceanogr.*, *16*, 1914-1928, 1996.

Moretti, M., E. Sansone, G. Spezie, and A. De Maio, Results of investigations in the Sicily Channel (1986-1990), *Deep Sea Res., Part A, 40*, 1181-1192, 1993.

Okkonen, S. R., Observations of topographic planetary waves in the Bering slope current using the Geosat altimeter, *J. Geophys. Res.*, *98*, 22,603-22,613, 1993.

Pedlosky, J., A study of the time dependent ocean circulation, *J. Atmos. Sci.*, *22*, 267-272, 1965.

Pedlosky, J., Fluctuating winds and the ocean circulation, *Tellus*, *19*, 250-256, 1967.

Pedlosky, J., *Geophysical Fluid Dynamics*, Springer-Verlag, New York, 1987.

Pierini, S., A divergent quasi-geostrophic model for wind-driven oceanic fluctuations in a closed basin, *Dyn. Atmos. Oceans*, *14*, 259-277, 1990. (Correction, *Dyn. Atmos. Oceans*, *14*, 415, 1990.)

Platzman, G. W., G. A. Curtis, K. S. Hansen, and R. D. Slater, Normal modes of the world ocean, II, Description of modes in the period range 8 to 80 hours, *J. Phys. Oceanogr.*, *11*, 579-603, 1981.

Ponte, R.M., The sea level response of a stratified ocean to barometric pressure forcing, *J. Phys. Oceanogr.*, *22*, 109-113, 1992.

Ponte, R.M., Variability in a homogeneous global ocean forced by barometric pressure, *Dyn. Atmos. Oceans*, *18*, 209-234, 1993.

Ripa, P., Normal Rossby modes of a closed basin with topography, *J. Geophys. Res.*, *83*, 1947-1957, 1978.

Thompson, R., Topographic Rossby waves at a site north of the Gulf Stream, *Deep Sea Res.*, *18*, 1-19, 1971.

Thompson, O. R. Y., and J. R. Luyten, Evidence for bottom-trapped topographic Rossby waves from single moorings, *Deep Sea Res.*, *23*, 629-635, 1976.

Zahel, W., The influence of ocean and solid earth parameters on oceanic eigenoscillations, tides and tidal dissipation, in Variations in Earth Rotation, *Geophys. Monogr. Ser.*, vol. 59, edited by D.D. McCarthy and W.E. Carter, pp. 33-41, AGU, Washington, D.C., 1990.

S. Pierini, Istituto di Meteorologia e Oceanografia, Istituto Universitario Navale, Corso Umberto I, 174 - 80138 Naples, Italy. (e-mail: pierini@naval.uninav.it)

(Received January 24, 1995; revised October 10, 1995; accepted October 12, 1995.)